MDPI

Article

Synthesis of Trivinylisooctyl POSS and Its Application in UV-Curing of Polyurethane Acrylate Coatings

Yufeng Wang [1,*]**, Zhenheng Cao** [2]**, Ziheng Wang** [1] **and Aijuan Ma** [1]

[1] School of Chemical and Chemical Engineering, Longdong University, Qingyang 745000, China; w15629627322@163.com (Z.W.); wangyiyouxiang1maj@163.com (A.M.)
[2] School of Chemistry and Chemical Engineering, Yan'an University, Yan'an 716000, China; hgjoys@126.com
[*] Correspondence: wesdxcqaz2004@126.com

Abstract: To improve the overall performance of polyurethane acrylic (PUAs) coatings applied to an iron or wood substrate, a modifier, trivinylisooctyl polyhedral oligomeric silsesquioxane (TVi^{7iso}–POSS), was successfully synthesized by a polycondensation reaction in the presence of an organotin catalyst. TVi^{7iso}–POSS is a POSS derivative possessing three olefin and seven isooctyl bonds; its molecular structure was confirmed by FT-IR, ^{1}H-NMR, and mass spectrometry. The synthesized TVi^{7iso}–POSS was then used as a modifier with butyl methacrylate (BMA), dodecafluoroheptyl methacrylate (DFMA), difunctional PUA (PUA–2), and photo-initiator 1173 to produce a novel polyurethane coating (PFMPUAs) via UV-curing. The performance of the obtained PFMPUAs coating was analyzed via X-ray photoelectron spectrometry, SEM, atomic force microscopy, TGA, and differential scanning calorimetry. The newly synthesized modifier, TVi^{7iso}–POSS, enhanced the thermal stability, hardness, flexibility, impact resistance, and adhesion of the PUAs coating and maintained its good light transmittance. Moreover, the PFMPUAs coating exhibited better overall performance compared to the previously studied PUAs coating when the addition of TVi^{7iso}–POSS and DFMA was 15 wt.% of PUA–2. Therefore, the PFMPUAs coating has potential applications in the field of environmentally friendly coatings.

Keywords: polyurethane acrylic resin; coating; POSS; flexibility; thermal stability

1. Introduction

The substrates of most metals or wood exposed to the natural environment are unavoidably affected by physical erosion, chemical degradation, temperature, humidity changes, light, and microorganisms, all of which accelerate ageing [1,2]. Therefore, some researchers have focused on developing environmentally friendly coatings to protect these substrates [3–6]. Among the various existing studies, organic coatings are widely used in the field of high-temperature and corrosion resistance of substrates because of their simple operation and cost-effectiveness [7–9].

Polyurethane acrylic resin (PUAs), a common organic coating, has received significant research attention. It can be used as a light-curing coating and is usually the first option for protecting iron or wood substrates [10]. However, the performance of UV-cured PUA coatings is poor in some areas [11], such as hardness, high-temperature resistance, outdoor aging resistance, adhesion, and flexibility, thereby limiting its applications. To improve the overall performance of the PUAs coating and expand its range of applications, a modifier is required. Typically, the performance of PUA coatings can be improved by adding other organic monomers or inorganic nanoparticles [12,13].

As an ideal organic and inorganic hybrid molecule, polyhedral oligomeric silsesquioxane (POSS) was incorporated into polyurethane to prepare a reinforced coating [14,15]. Therefore, studies typically use POSS of a single functional group or eight functional groups to modify PUAs coatings. Some studies have confirmed that a single functional POSS can

improve the thermal stability of the PUAs coating; however, its hardness and mechanical performance remain unsatisfactory [16]. When the PUAs coating is modified by the eight functional groups of POSS, its hardness improves; however, its flexibility and adhesion become worse owing to its significant cross-chain effect.

It can be concluded that neither the single functional POSS nor the eight functional groups of POSS are an ideal modifier because each of them improves the performance of the PUAs coatings in certain aspects; however, they also introduce certain disadvantages. Consequently, a new idea was considered, which involved combining their advantages and overcoming their disadvantages. Experiments were designed and conducted to determine an optimal method for POSS to modify the PUAs coating–trifunctional group POSS.

The trials were divided into two parts. First, trivinylisooctyl POSS (TVi^{7iso}–POSS) was synthesized using a semi-closed cage trisilanolisooctyl POSS ($TSiOH^{7iso}$–POSS) and ethoxydimethylvinylsilane (EMVS). TVi^{7iso}-POSS, the trifunctional group POSS, was employed to modify the PUAs coating. TVi^{7iso}-POSS possesses three olefin and seven isooctyl bonds. The three olefin bonds polymerize in three directions, which can enhance the hardness of the coating and maintain its degree of crosslinking. The seven isooctyl bonds can increase the solubility of the coating, which enhances its flexibility. Moreover, TVi^{7iso}–POSS exhibits a cage structure, which can increase the hardness and thermal stability of the coating. Therefore, PUA coatings modified by TVi^{7iso}–POSS are expected to have good flexibility, adhesion, hardness, and high-temperature resistance.

2. Experimental Section

2.1. Raw Materials

Trisilanolisooctyl POSS ($TSiOH^{7iso}$–POSS) was purchased from Hybrid Plastics, Hattiesburg, CA, USA. Ethoxydimethylvinylsilane (EMVS) was supplied by Merck Co., Ltd., Shanghai, China. Dibutyltin dilaurate (DBTDL) and butyl methacrylate (BMA) were purchased from Hangzhou Xinbao Chemical Co., Ltd. (Hangzhou, China) and Tianjin Fuchen Chemical Reagent Co., Ltd. (Tianjin, China), respectively. Dodecafluoroheptyl methacrylate (DFMA) was obtained from Silword Chemical Co., Ltd., Wuhan, China. The difunctional polyurethane acrylate (PUA–2) is a PUA with two olefin-based groups, obtained from Shanghai Yinchang New Materials Co., Ltd (Shanghai, China). Tetrahydrofuran (THF) was provided by Fuchen Chemical Reagent Co., Ltd., Tianjin, China. Photo-initiator 1173 was purchased from Mingda Macromolecule Science and Technology Co., Ltd., Suzhou, China. In addition to these chemical materials, tin plates were employed as the substrates and cut into 150 mm × 75 mm samples, all of which were polished with abrasive paper (No. 80) and washed in deionized water and absolute alcohol successively before painting. The full names and corresponding abbreviations of the raw materials, including synthetic products, are listed in Table 1.

Table 1. Full name and abbreviation contrast diagram.

Full Name	Abbreviation	Full Name	Abbreviation
Trisilanolisooctyl POSS	$TSiOH^{7iso}$–POSS	Ethoxydimethylvinylsilane	EMVS
Dibutyltin dilaurate	DBTDL	Butyl Methacrylate	BMA
Polyurethane acrylate	PUA	Difunctional Polyurethane acrylate	PUA–2
Dodecafluoroheptyl methacrylate	DFMA	Polyurethane acrylic resin	PUAs
Tetrahydrofuran	THF	Photo-initiator 1173	1173
Trivinylisooctyl POSS	TVi^{7iso}–POSS	The PUAs coating modified by TVi^{7iso}-POSS and DFMA	PFMPUAs

2.2. Synthesis of TVi^{7iso}–POSS

In a three-neck flask equipped with a mechanical stirrer, reflux condenser, and thermometer, EMVS was dissolved in THF, and two drops of DBTDL were added as the catalyst. The mixture was stirred and heated to 40 °C. Trisilanolisooctyl POSS ($TSiOH^{7iso}$–POSS) was then dissolved in THF and added dropwise into the flask. The entire dripping process

lasted for 1 h. The molar ratio of EMVS to TSiOH^{7iso}–POSS was 3:1. The reaction was conducted continuously for 48 h at a constant temperature. After the reaction ended, and the product was distilled and dried under vacuum, a new POSS derivative, trivinylisooctyl POSS (TVi^{7iso}–POSS), was obtained. It comprised three olefin and seven isooctyl bonds. The reaction equation is shown in Scheme 1, where the R group denotes isooctyl.
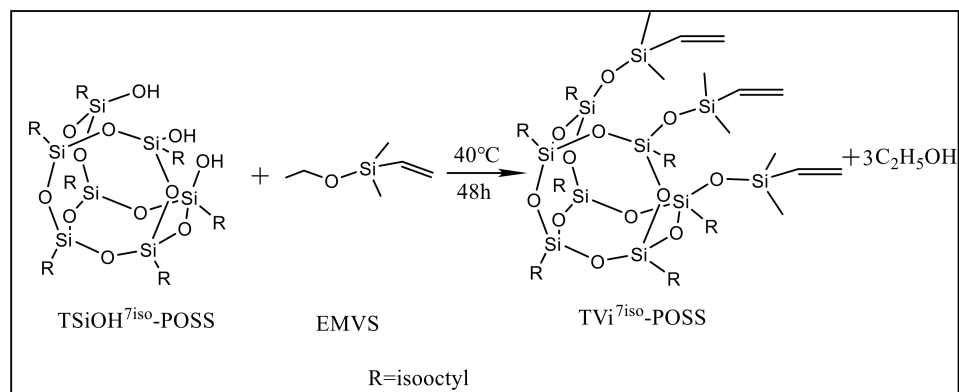
Scheme 1. Synthesis of TVi^{7iso}–POSS.

2.3. Preparation of the PFMPUAs Coating

PUA-2, TVi^{7iso}–POSS, DFMA, BMA, and photo-initiator 1173 were mixed evenly in a mass ratio of 100:15:15:3:3 and kept for approximately 3–5 min to remove the bubbles. Subsequently, the mixture was coated onto a tin plate to form a wet film and kept for approximately 3–5 min. Subsequently, it was placed in a UV-curing machine and exposed to UV light (360 nm) for 1 min to obtain the PUAs coating (PFMPUAs) modified by TVi^{7iso}–POSS and DFMA. The UV-curing process of the PFMPUAs coating is shown in Scheme 2.
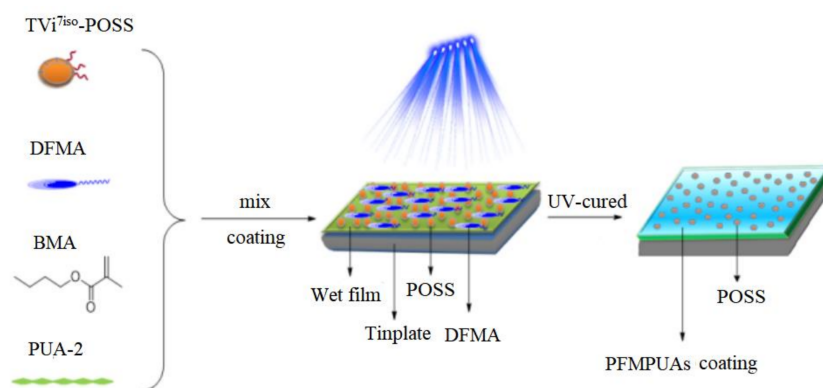
Scheme 2. Preparation of the PFMPUAs coating.

2.4. Characterization

First, the molecular structure of TVi^{7iso}–POSS was characterized using Fourier-transform infrared spectrometry (FT-IR), proton nuclear magnetic resonance spectroscopy (^{1}H-NMR), and mass spectrometry (MS). The infrared spectrum was examined using a Fourier-transform infrared (FT-IR) spectrum analyzer (SHIMADZU IRTracer-100 spectrometer, Kyoto, Japan). Proton nuclear magnetic resonance spectroscopy (^{1}H-NMR) spectra were obtained using a 400 MHz NMR spectrometer (Bruker, Karlsruhe, Germany) with (methyl sulfoxide)-D6 as the solvent. MS analysis was performed using a Bruker Autoflex max MALDI-TOF mass spectrometer (Bruker, Karlsruhe, Germany). Second, the surface composition of the coating was investigated using an Axis Ultra X-ray photoelectron spectrometer (XPS) (Kratos, Manchester, UK). Third, the surface morphology of the coating was observed using atomic force microscopy (AFM) (Bruker Dimension ICON, Karlsruhe, Germany).

Finally, the thermal and mechanical performances of the PFMPUAs coating were characterized, including the thermostability, hardness, impact resistance, adhesion, flexibility, and hydrophobicity.

The thermostability of the coating was measured under nitrogen using a Q500 thermogravimetric analyzer (TA, New Castle, DE, USA) at a heating rate of 20 °C/min. The hardness of the coating was tested using the XQ-QHQ manual pencil hardness tester at Dongguan Xingqiao Instrument Equipment Co., Ltd. (Dongguan, China), Guangdong, and the method is detailed in the national standard GB/T6 739-2006. The impact resistance of the coating was measured using a QCJ paint film impact testing machine (Shanghai Leao Test Instrument Co., Ltd., Shanghai, China). Coating adhesion was observed using a film adhesion tester (Changzhou Detu Precision Instrument Co., Ltd., Changzhou, China). A rotary needle was used to scratch the paint film to determine the adhesion of the coating according to the national standard GB 1720–1979, China. The flexibility of the coating was determined using a QTY-32 paint film bending tester (Shanghai Meizu Instrument Co., Ltd., Shanghai, China); the detailed process can be found in the national standard GB/T 1731-93. The hydrophobicity of the coating was determined via the static water contact angle (WCA) method on a tinplate using SDC-80 contact angle goniometer (Shengding Precision Instrument Co., Ltd., Dongguan, China) at 20 °C. In this method, the liquid volume was 5 μL and the average of five readings from different regions of the same sample was used as the final result for each sample.

3. Results and Discussion

3.1. Structural Characterization of TVi^{7iso}–POSS

To confirm the molecular structure of the synthesized TVi^{7iso}–POSS, its FT–IR, ^{1}H-NMR, and mass spectra were obtained.

The FT-IR spectra of Tvi^{7iso}-POSS, TsiOH^{7iso}-POSS, and EMVS are shown in Figure 1. In the FT-IR spectra of TsiOH^{7iso}-POSS, the peak at 2900 cm^{-1} is mainly related to the (–CH$_2$–) and (–CH$_3$) groups of isooctyl from the POSS vertices. The large peak at approximately 1100 cm^{-1} is the stretching vibration peak of the (Si–O–Si) groups on POSS. The peak at 3300 cm^{-1} is the vibration absorption peak of (Si–OH). In the FT-IR spectra of EMVS, the small peak at 3100 cm^{-1} is the (=C–H) peak of EMVS. In the FT-IR spectra of Tvi^{7iso}–POSS, the peaks at 1680–1630 cm^{-1} and at 917 cm^{-1} correspond to the stretching vibration of alkenyl C=C and the bend vibration of =C-H, respectively, and the peak at 3100 cm^{-1} corresponds to the stretching vibration of (=C–H), which indicates that the double bond was successfully introduced into TVi^{7iso}-POSS. The vibration absorption peak of (Si–OH) nearly disappeared at 3300 cm^{-1}, indicating that TSiOH^{7iso}-POSS reacted completely. Hence, it can be concluded that TVi^{7iso}-POSS was obtained.
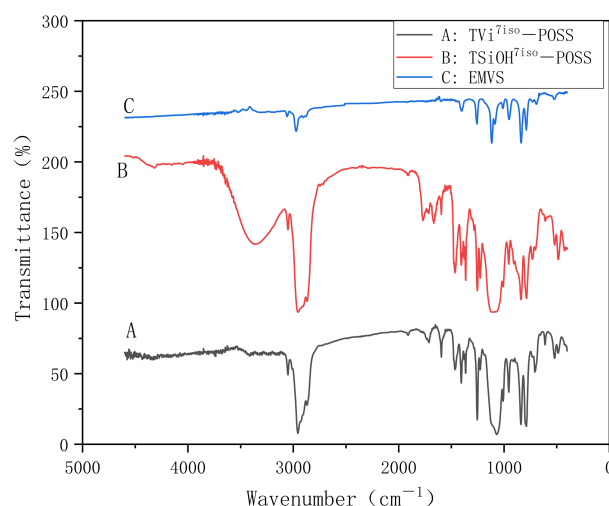
Figure 1. FT-IR spectra of TVi^{7iso}–POSS.

To further determine the structure of TVi[7iso]–POSS, its ^{1}H–NMR spectra were investigated and compared to that of TSiOH[7iso]-POSS. Figure 2A shows the ^{1}H-NMR spectra of TSiOH[7iso]–POSS. It can be observed that the peak at 2.54 ppm is the solvent peak of the deuterated DMSO, and the peak at 3.33 ppm is the residual water peak in the deuterated DMSO. The peaks at 6.50 ppm are the (Si–OH) peaks of TSiOH[7iso]–POSS. Figure 2B shows the peaks of the reaction product TVi[7iso]-POSS. In the figure, the multi-peaks (approximately seven or eight peaks) at 5.55 to 6.00 ppm are the characteristic peaks of (–CH–) and (–CH$_2$–) of (–CH=CH$_2$) on TVi[7iso]–POSS. The peaks at 0.70 to 2.00 ppm are the characteristic peaks of (–CH–), (–CH$_2$–), and (–CH$_3$) of isooctyl. The peak of (Si–OH) at 6.50 ppm disappeared, and the ethanol peak appeared at 3.44 ppm. These results indicate that the reaction was complete, and the final product was TVi[7iso]-POSS.
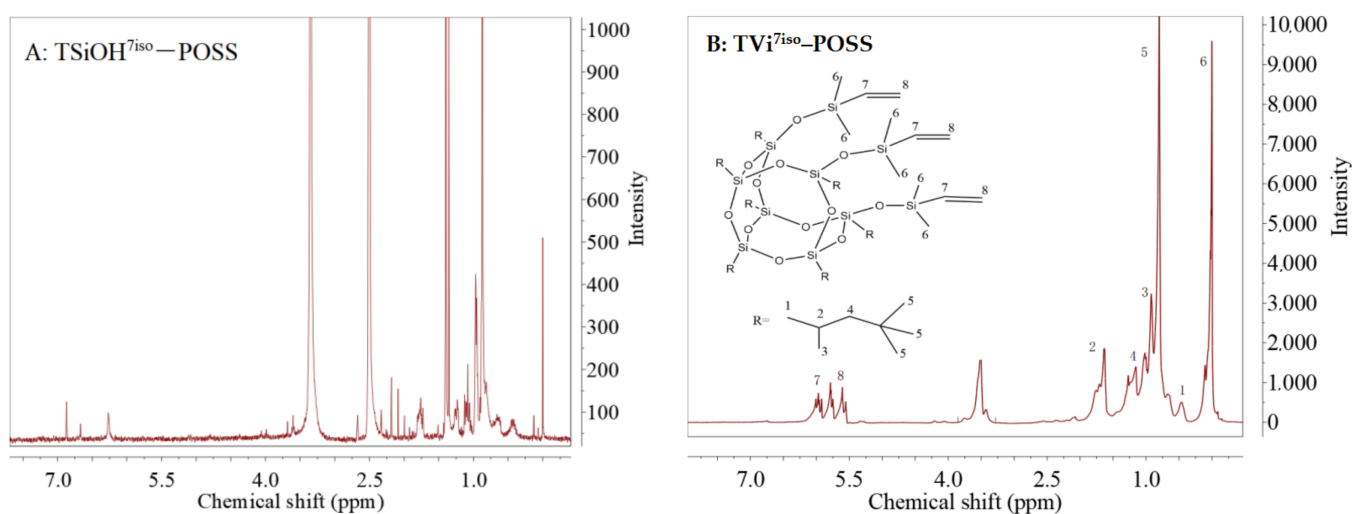
Figure 2. ^{1}H–NMR spectra of TSiOH[7iso]–POSS (**A**) and TVi[7iso]–POSS (**B**).

A mass spectrum was also obtained, as shown in Figure 3. The sum of the measured molecular weights was equal to the expected molecular weight. This indicates that TSiOH[7iso]-POSS reacted successfully and completely. The obtained TVi[7iso]–POSS appeared pale yellow, as shown in Figure 4.
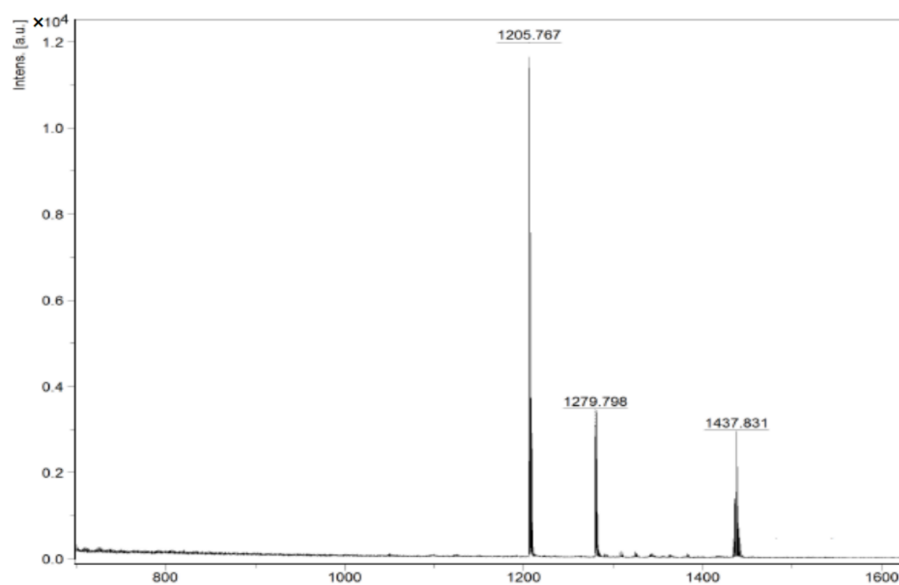
Figure 3. Mass spectra of TVi[7iso]–POSS.

Figure 4. Appearance of TVi^{7iso}–POSS.

3.2. Composition Characterization of the PFMPUAs Coating

To understand the chemical composition of the PFMPUAs coating, XPS was used to characterize the presence of main elements such as C, Si, F, and O [17,18]. The wide scanning and high-resolution spectra of the PFMPUAs coating are shown in Figure 5.
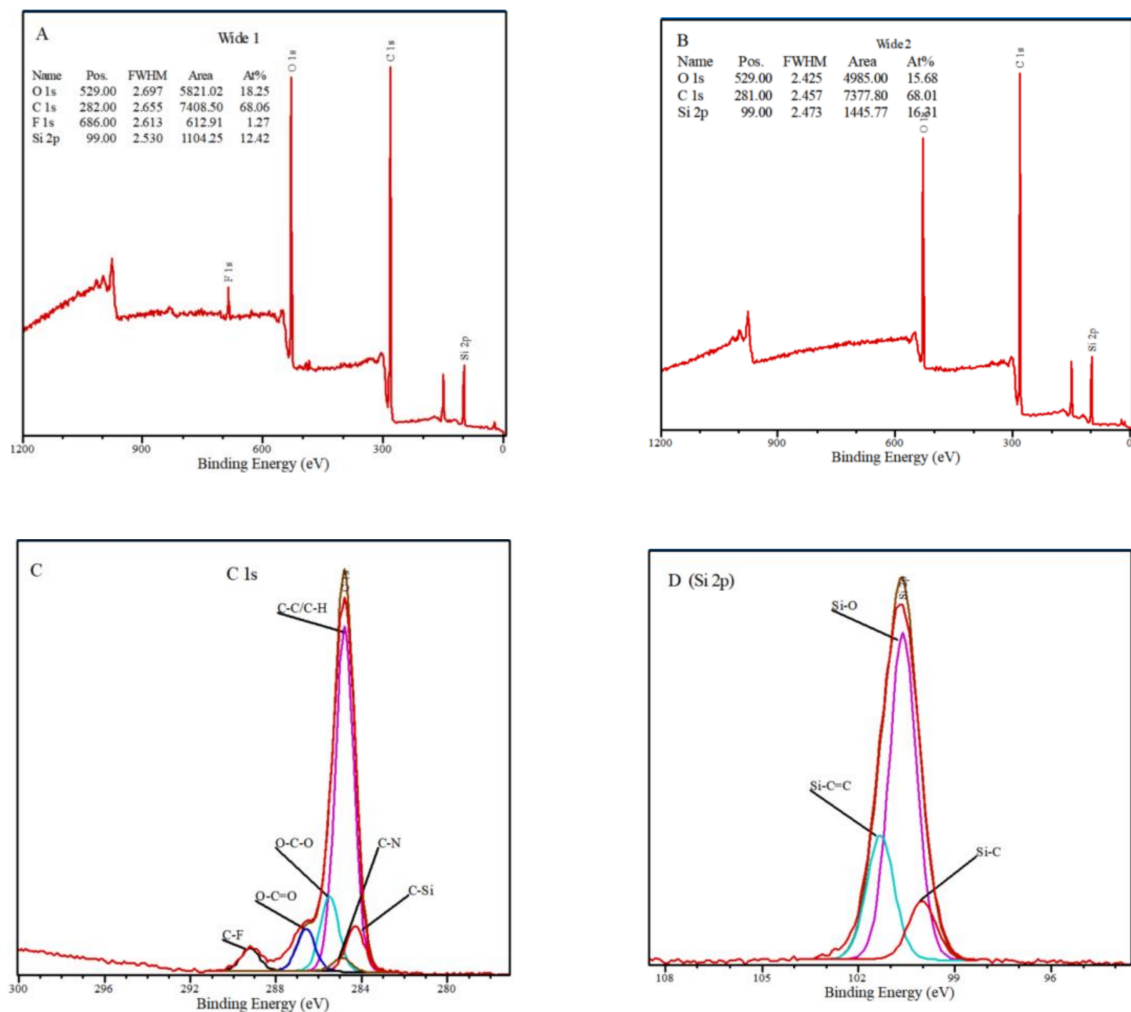
Figure 5. XPS spectra of the PFMPUAs coating: (**A**) wide 1 scanning; (**B**) wide 2 scanning; (**C**) C 1s; (**D**) Si 2p.

The wide spectra of the surface and back of the coating are shown in Figure 5A,B, respectively. In Figure 5A, four elements, C, Si, F and O, are observed on the surface of the coating, occurring at binding energies of 283.00 (C 1s), 100.00 (Si 2p), 686.87 (F 1s), and 530.39 eV (O 1s), whereas nitrogen peaks at 397.70 eV (N 1s) were not observed, because nitrogen functions as a skeleton in the coating and is mainly distributed in the inner coating. Furthermore, only three elements (C, Si, and O) were observed in Figure 5B. The fluoride monomer grafts to the molecular chain when the coating is cured, and the fluorinated group moves toward the upper surface of the coating and plays a hydrophobic role; therefore, there is no fluorine deposition on the back of the coating. The mechanism of the fluorine group shifting to the surface of the coating was not investigated further in this study; however, it is necessary to investigate it in detail in future studies. The presence of Si was owing to the introduction of TVi^{7iso}-POSS into the coating.

The high-resolution spectra of the coating are shown in Figure 5C,D, which exhibit the following peaks. The C1s spectrum in Figure 5C exhibits several splitting peaks: at 284.34 eV for the (C–Si) bond, 284.84 eV for the (C–C/C–H) bond, 284.89 eV for the (C–N) bond, 285.53 eV for the (O–C–O) bond, 286.62 eV for the (O–C=O) bond, and 289.27 eV for the (C–F) bond. The Si 2p spectrum in Figure 5D consisted of three identical fitting peaks with binding energies of 100.06 (Si–C), 100.63 (Si–O), and 101.37 eV (Si–C=C). Thus, it can be concluded that DFMA and TVi^{7iso}-POSS successfully participated in the UVcuring reaction, and F atoms migrated to the surface of the coating and played a hydrophobic role.

3.3. Surface Morphology of the PFMPUAs Coating

To determine the surface morphology of the PFMPUAs coating, AFM images (3D graph and topography) of the coating were studied; they are shown in Figure 6. It was observed from the topography image that several nanoparticles were evenly dispersed on the surface of the coating, whereas in the 3D graph, the surface was rough and uneven from a micro perspective. This is because TVi^{7iso}–POSS includes not only nano-sized cage-like POSS but also three olefin bonds, which are adequate to polymerize with other olefins from branched chains to form large nanometer or micron bumps on the surface.

(A)   (B)
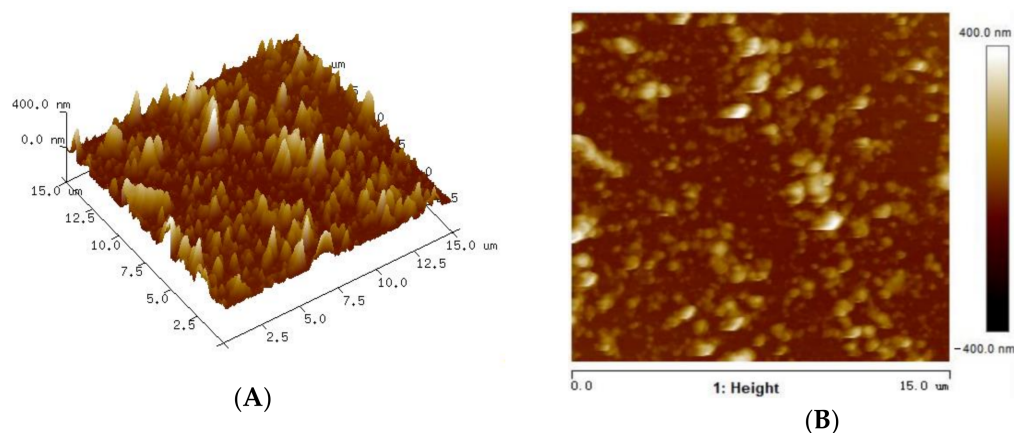
Figure 6. AFM images on a silicon wafer of coating: (**A**) 3D graph and (**B**) topography.

3.4. Thermal Performance Characterization of the PFMPUAs Coating

Thermogravimetric analysis (TGA) was performed to evaluate thermal stability by investigating the weight loss of the material against temperature. Differential scanning calorimetry (DSC) was also performed.

TGA thermograms of the PFMPUA coatings with different TVi^{7iso}-POSS contents (ranging from 2 to 20 wt.% of PUA-2) are shown in Figure 7A. It can be observed that all TGA thermograms exhibit similar degradation behaviors, which can be explained by three stages. The first stage (<200 °C) is attributed to the volatilization of small molecules (such as DFMA and photo-initiator 1173) and moisture in the coating. The second stage (200–400 °C)

can be regarded as the decomposition temperature of the hard section. The third stage (400–580 °C) is owing to the decomposition of the soft section and cross-linked bonds. The decomposition temperature of the PFMPUAs coatings with different TVi[7iso]–POSS contents varied from 285 to 311 °C when the mass loss was 10%, whereas it improved from 385 to 395 °C when the mass loss was 50% and reached 465 to 559 °C when the mass loss was 80%. In addition, it was also observed that the decomposition process at 285–400 °C for all coatings occurred at maximum rates, and its mass loss increased from 10 to 60%. The final residual amount of the coating after decomposition increased as the TVi[7iso]–POSS content increased and peaked when the TVi[7iso]–POSS content increased to 20 wt.%. Thus, the introduction of TVi[7iso]–POSS can increase the thermal stability of the coating.
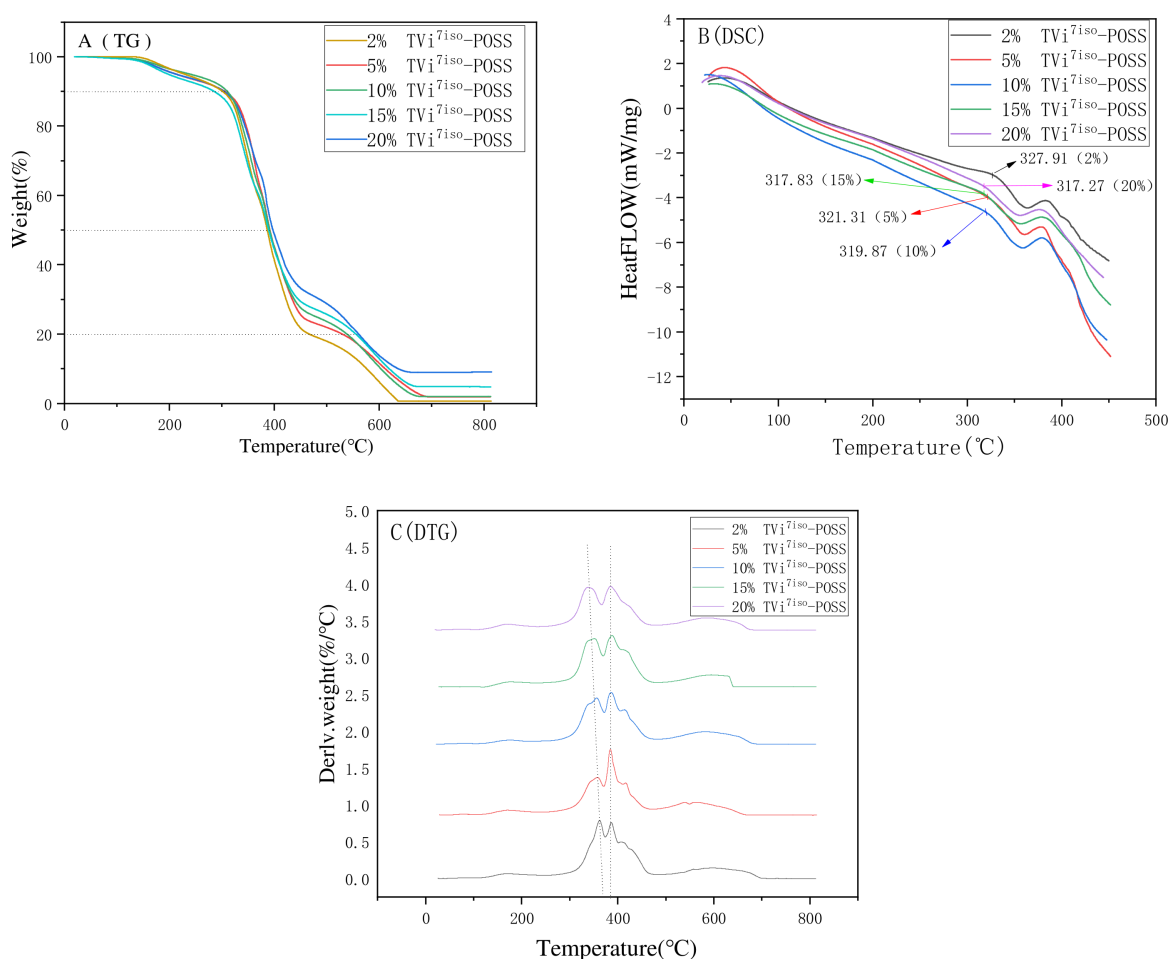
Figure 7. TGA, DSC, and DTG thermograms of the PFMPUA coatings with different TVi[7iso]–POSS contents. (**A**) TGA thermograms; (**B**) DSC thermograms of the coating; (**C**) DTG thermograms.

To further confirm the better thermal stability of the PFMPUAs coatings, DSC and derivative thermogravimetry (DTG) thermograms of the coatings with different TVi[7iso]–POSS percentages (2–20 wt.% of PUA-2) were investigated separately, and are presented in Figure 7B,C. It can be observed that the T_g decreased from 327.91 to 317.27 °C with increasing TVi[7iso]–POSS, and the rate decreased as the TVi[7iso]–POSS approached 20 wt.%. This is because the PFMPUAs coating is a hot-curing coating, and its crosslinking degree increases as the TVi[7iso]-POSS content increases. However, because TVi[7iso]–POSS possesses seven isooctyl bonds, its introduction reduces the T_g of the PFMPUAs coating [19,20]. When the amount of TVi[7iso]–POSS continued to increase, the crosslinking degree increased further, restricting the isooctyl bond movements; thus, the T_g gradually stabilized. This demonstrates the increase in flexibility with increasing TVi[7iso]–POSS.

3.5. Hydrophobicity Characterization of the PFMPUAs Coating

The hydrophobicity of coatings is an indispensable factor for practical applications [21,22]. In this study, DFMA can reduce the surface free energy of the coating to improve its hydrophobicity, which was used as the main material with TVi^{7iso}–POSS to prepare the PFMPUAs coating. To determine the influence of its content on the hydrophobicity of the PFMPUAs coating, a series of coatings was synthesized by only varying the amount of DFMA (2–25 wt.% of PUA-2), while keeping the amount of the other raw materials constant. Figure 8 shows the WCAs of the synthesized PFMPUAs coatings. Overall, the WCAs of the coatings initially increased and then decreased with an increase in the DFMA content. This is because the fluorine groups in the polymer preferentially migrated to and accumulated on the surface of the coating during the UV-curing process, which results in a decrease in the surface free energy of the coating, until the fluoride groups tend to saturate. Furthermore, it is also clear that the PFMPUAs coating exhibits better hydrophobicity and light transmittance when the DFMA content is 15 wt.%, because the PFMPUAs films exhibit the highest WCA (105°) at that point.
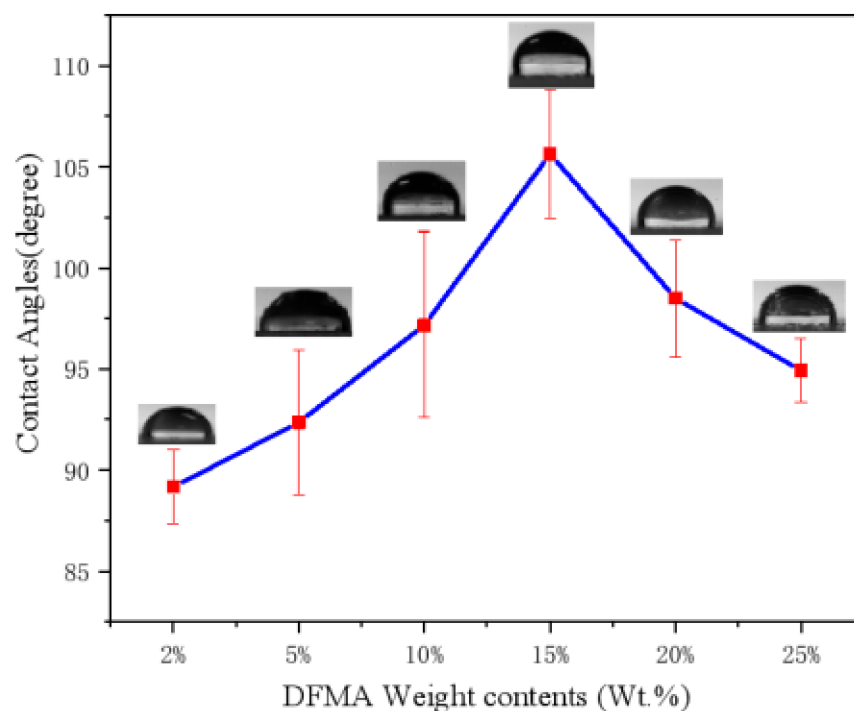
Figure 8. Influence curves of TVi^{7iso}-POSS amount on the contact angle of the coating.

3.6. Mechanical Performance Characterization of the PFMPUAs Coating

Mechanical performance is an important parameter of coatings, and TVi^{7iso}–POSS as an inorganic nanomaterial can affect it directly; therefore, studies on the mechanical performance of PFMPUAs coatings are necessary, including the adhesion grades, hardness, flexibility, and impact resistance. The results are listed in Table 2. It is evident that the hardness, adhesion, and flexibility of the PFMPUAs coating increased with an increase in the TVi^{7iso}–POSS content. This was because TVi^{7iso}-POSS possesses only three olefin bonds. Crosslinking occurs only in three directions in the polymerization process; therefore, its crosslinking degree is lower than that of octa functional olefin bonds [16]. From physical analysis, the POSS of TVi^{7iso}-POSS can be viewed as anchor points, which can increase the hardness and adhesion of the coating. Consequently, it can be concluded from Table 2 that the mechanical properties of the PFMPUAs coating are better when the amount of TVi^{7iso}–POSS is 15 wt.%.

Table 2. Effect of TVi^{7iso}-POSS content on the mechanical performance of the PFMPUAs coating.

TVi^{7iso}-POSS Percentage of PUA-2 (wt.%)	0	2	5	10	15	20
adhesion grades	7	3	2	1	1	2
hardness	H	2H	4H	5H	6H	6H
flexibility (cm)	φ15	Φ10	Φ5	Φ5	Φ4	Φ4
impact resistance (cm)	45	45	50	55	55	50

3.7. Light Transmittance Characterization of the PFMPUAs Coating

The light transmittance of PFMPUAs coated with 15 wt.% TVi^{7iso}–POSS was investigated. The results indicated that the light transmittance of the unmodified PUAs coating was 98%, whereas that of the PFMPUAs coating was close to 95%. This indicates that the PFMPUAs coating has similar light transmittance as the blank PUAs coating. This is because the vertex of the POSS cage on TVi^{7iso}–POSS possesses seven isooctyl bonds, which improves the solubility of the PFMPUAs coating. Therefore, the PFMPUAs coating with 15 wt.% TVi^{7iso}-POSS exhibited good mechanical performance and excellent light transmittance.

4. Conclusions

A novel POSS derivative, trivinylisooctyl POSS (TVi^{7iso}–POSS), was successfully synthesized by the polycondensation of ethoxydimethylvinylsilane (EMVS) and trisilanolisooctyl POSS (TSiOH^{7iso}–POSS), and then incorporated into a PUAs coating to obtain a PFMPUAs coating via UV-curing. The synthetic TVi^{7iso}-POSS not only improved the hardness and thermal stability of the PUAs coating but also improved its flexibility. In particular, when the content of TVi^{7iso}–POSS was 15 wt.%, the PFMPUAs coating exhibited better overall performance compared with previous coatings modified by the single functional POSS or eight functional groups of POSS. Furthermore, the hydrophobicity was improved, and the WCA was 105° when the dodecafluoroheptyl methacrylate (DFMA) was 15 wt.%. Therefore, the modified PFMPUAs coating exhibited a better overall performance. In addition, the mechanism of the fluorine group shifting to the surface of the coating would be investigated in detail in future studies.

Author Contributions: Conceptualization, A.M.; Data curation, Y.W., Z.C., Z.W. and A.M.; Formal analysis, Z.C.; Funding acquisition, Y.W.; Investigation, Z.W.; Project administration, Y.W.; Writing—original draft, Y.W. All authors have read and agreed to the published version of the manuscript.

Institutional Review Board Statement: Not applicable.

Informed Consent Statement: Not applicable.

Data Availability Statement: Not applicable.

Conflicts of Interest: The authors declare no conflict of interest.

References

1. Sultan, S.; Kareem, K.; Ling, H. Synthesis, Characterization and Resistant Performance of α-Fe$_2$O3@SiO$_2$ Composite as Pigment Protective Coatings. *Surf. Coat. Technol.* **2016**, *300*, 42–49. [CrossRef]
2. Xu, J.; Jiang, Y.; Zhang, T.; Dai, Y.; Yang, D.; Qiu, F.; Yu, Z.; Yang, P. Fabrication of UV-Curable Waterborne Fluorinated Polyurethane-Acrylate and Its Application for Simulated Iron Cultural Relic Protection. *J. Coat. Technol. Res.* **2018**, *15*, 535–541. [CrossRef]
3. Al Kindi, M.; Joshi, G.R.; Cooper, K.; Andrews, J.; Arellanes-Lozada, P.; Leiva-Garcia, R.; Engelberg, D.L.; Bikondoa, O.; Lindsay, R. Substrate Protection with Corrosion Scales: Can We Depend on Iron Carbonate? *ACS Appl. Mater. Interfaces* **2021**, *13*, 58193–58200. [CrossRef]
4. Xian, L.; Zhao, H.; Xian, G.; Wang, C.; He, H. High Temperature Protection of NiCrAlSiY/Al–Cr–O Coatings Deposited by Arc Ion Plating on Nickel-Based Superalloy. *Vacuum* **2021**, *188*, 110152. [CrossRef]

5. Cui, M.; Njoku, D.I.; Li, B.; Yang, L.; Li, Y. Corrosion Protection of Aluminium Alloy 2024 through an Epoxy Coating Embedded with Smart Microcapsules: The Responses of Smart Microcapsules to Corrosive Entities. *Corros. Commun.* **2021**, *1*, 1–9. [CrossRef]

6. Duan, Y.; Wu, Y.; Yan, R.; Lin, M.; Ma, H. Chitosan-Sodium Alginate-Based Coatings for Self-Strengthening Anticorrosion and Antibacterial Protection of Titanium Substrate in Artificial Saliva. *Int. J. Biol. Macromol.* **2021**, *184*, 109–117. [CrossRef]

7. Ahmetli, G.; Deveci, H.; Soydal, U.; Seker, A.; Kurbanli, R. Coating, Mechanical and Thermal Properties of Epoxy Toluene Oligomer Modified Epoxy Resin/Sepiolite Composites. *Prog. Org. Coat.* **2012**, *75*, 97–105. [CrossRef]

8. Zheng, H.; Liu, G.; Nienhaus, B.B.; Buddingh, J. V Ice-Shedding Polymer Coatings with High Hardness but Low Ice Adhesion. *ACS Appl. Mater. Interfaces* **2022**, *14*, 6071–6082. [CrossRef]

9. Chen, K.; Liu, H.; Zhou, J.; Sun, Y.; Yu, K. Polyurethane Blended with Silica-Nanoparticle-Modified Graphene as a Flexible and Superhydrophobic Conductive Coating with a Self-Healing Ability for Sensing Applications. *ACS Appl. Nano Mater.* **2022**, *5*, 615–625. [CrossRef]

10. Zhang, X.; Lin, D.; Liu, Z.; Yuan, S.; Wang, X.; Wang, H.; Wang, J. Fabrication of Mechanically Stable UV-Curing Superhydrophobic Coating by Interfacial Strengthening Strategy. *J. Alloys Compd.* **2021**, *886*, 161156. [CrossRef]

11. Ning, F.; He, G.; Sheng, C.; He, H.; Wang, J.; Zhou, R.; Ning, X. Yarn on Yarn Abrasion Performance of High Modulus Polyethylene Fiber Improved by Graphene/Polyurethane Composites Coating. *J. Eng. Fiber. Fabr.* **2021**, *16*, 1558925020983563. [CrossRef]

12. Fu, J.; Yu, H.; Wang, L.; Liang, R.; Zhang, C.; Jin, M. Preparation and Properties of UV-Curable Polyurethane Acrylate/SiO$_2$ Composite Hard Coatings. *Prog. Org. Coat.* **2021**, *153*, 106121. [CrossRef]

13. Wang, X.; Cui, Y.; Wang, Y.; Ban, T.; Zhang, Y.; Zhang, J.; Zhu, X. Preparation and Characteristics of Crosslinked Fluorinated Acrylate Modified Waterborne Polyurethane for Metal Protection Coating. *Prog. Org. Coat.* **2021**, *158*, 106371. [CrossRef]

14. Zhang, S.; Zou, Q.; Wu, L. Preparation and Characterization of Polyurethane Hybrids from Reactive Polyhedral Oligomeric Silsesquioxanes. *Macromol. Mater. Eng.* **2010**, *291*, 895–901. [CrossRef]

15. Oaten, M.; Choudhury, N.R. Silsesquioxane−Urethane Hybrid for Thin Film Applications. *Macromolecules* **2005**, *38*, 6392–6401. [CrossRef]

16. Wang, Y.; An, Q.; Yang, B. Synthesis of UV-Curable Polyurethane Acrylate Modified with Polyhedral Oligomeric Silsesquioxane and Fluorine for Iron Cultural Relic Protection Coating. *Prog. Org. Coat.* **2019**, *136*, 105235. [CrossRef]

17. Martinelli, E.; Glisenti, A.; Gallot, B.; Galli, G. Surface Properties of Mesophase-Forming Fluorinated Bicycloacrylate/Polysiloxane Methacrylate Copolymers. *Macromol. Chem. Phys.* **2010**, *210*, 1746–1753. [CrossRef]

18. Wei, X.U.; Qiufeng, A.N.; Hao, L.; Dan, Z.; Min, Z. Synthesis and Characterization of Self-Crosslinking Fluorinated Polyacrylate Soap-Free Latices with Core—Shell Structure. *Appl. Surf. Sci.* **2013**, *268*, 373–380. [CrossRef]

19. Mihelčič, M.; Gaberšček, M.; Luna, M.; Lavorgna, M.; Surca, A.K. Effect of Silsesquioxane Addition on the Protective Performance of Fluoropolymer Coatings for Bronze Surfaces. *Mater. Des.* **2019**, *178*, 107860. [CrossRef]

20. Fina, A.; Tabuani, D.; Frache, A.; Camino, G. Polypropylene–Polyhedral Oligomeric Silsesquioxanes (POSS) Nanocomposites. *Polymer* **2005**, *46*, 7855–7866. [CrossRef]

21. Zhao, B.; Jia, R. Preparation of Super-Hydrophobic Films Based on Waterborne Polyurethane and Their Hydrophobicity Characteristics. *Prog. Org. Coat.* **2019**, *135*, 440–448. [CrossRef]

22. Ding, G.; Jiao, W.; Chen, L.; Yan, M.; Hao, L.; Wang, R. A Self-Sensing, Superhydrophobic, Heterogeneous Graphene Network with Controllable Adhesion Behavior. *J. Mater. Chem. A* **2018**, *6*, 16992–17000. [CrossRef]